UNDER PEER REVIEW

[Original Research Article]

Superconvergence Analysis of Area-Weighted Gradient Recovery for Linear Elasticity Eigenvalue Problems

Abstract

This paper investigates area-weighted gradient recovery for two-dimensional linear elasticity eigenvalue problems. Based on conforming linear finite elements, a nodal area-weighted recovery operator is defined for the piecewise constant displacement gradient. Under suitable regularity assumptions, local approximate parallelogram conditions, a measure bound for the irregular region, and a local quadratic moment condition, we establish a sequence of estimates for the recovered gradient. In particular, we first prove a weak superapproximation estimate for the elasticity bilinear form and derive a supercloseness estimate between the finite element eigenfunction and the nodal interpolant of the exact eigenfunction. These results, together with a local recovery estimate, yield the global superconvergence bound

$$\|G_h[\nabla u_h] - \nabla u\|_{0,\Omega} \leq Ch^{1+\alpha_0}.$$

Numerical illustrations on an L-shaped domain compare the original and recovered gradient fields and report the behavior of a gradient recovery difference along an existing adaptive mesh sequence. Because the L-shaped domain has a reentrant-corner singularity and the adaptive meshes are locally nonuniform, these computations are presented as illustrations of recovery behavior rather than as a direct verification of the theoretical rate under all assumptions of the superconvergence theorem.

Keywords: linear elasticity eigenvalue problem; area-weighted gradient recovery; weak superapproximation; supercloseness; superconvergence; linear finite elements.

2010 Mathematics Subject Classification: [Not supplied]

1 Introduction

Linear elasticity eigenvalue problems describe free vibrations of elastic bodies. For finite element spectral approximation, see Boffi Boffi (2010) and the spectral approximation theory of Babuška and Osborn Babuška and Osborn (1991). Conforming linear finite elements yield piecewise constant, discontinuous displacement gradients. Improving these gradients benefits strain and stress approximation.

Gradient recovery is a widely used postprocessing technique for improving derivative approximations. The superconvergent patch recovery method of

Zienkiewicz and Zhu provides a classical framework for constructing recovered derivatives and a posteriori error estimates Zienkiewicz and Zhu (1992). On mildly structured triangulations, Bank and Xu Bank and Xu (2003) and Xu and Zhang Xu and Zhang (2004) established superconvergence and recovery estimates under local mesh-structure conditions. Related recovery analyses have also been developed for anisotropic meshes by Cao Cao (2014), while Shi, Xu, and Zhang studied recovery of elastic stresses on quadrilateral meshes Shi et al. (2008).

The present paper focuses on area-weighted nodal recovery of the displacement gradient for two-dimensional linear elasticity eigenvalue problems discretized by conforming piecewise linear triangular elements. The analysis combines the local approximate parallelogram structure of the triangulation with a measure condition on the irregular region. In addition, a local quadratic moment condition is imposed on regular nodal patches to control the recovery error for the quadratic term in the Taylor expansion. Under these assumptions, we establish a global superconvergence estimate for the recovered finite element gradient.

The main contributions are as follows. First, we define a componentwise area-weighted recovery operator for piecewise constant matrix-valued gradients and prove its L^2 stability. Second, by expressing the elasticity bilinear form componentwise and applying the scalar weak superapproximation estimate of Xu and Zhang Xu and Zhang (2004), we derive a weak superapproximation estimate for the elasticity problem and a supercloseness estimate between the discrete eigenfunction and the nodal interpolant of the exact eigenfunction. Third, using the local quadratic moment condition and separating regular and irregular recovery regions, we prove the global estimate

$$\|G_h[\nabla u_h] - \nabla u\|_{0,\Omega} \le Ch^{1+\alpha_0}.$$

The remainder of the paper is organized as follows. Section 2 introduces the continuous linear elasticity eigenvalue problem and its conforming finite element approximation. Section 3 defines the area-weighted recovery operator and establishes its stability. Section 4 proves the weak superapproximation and eigenfunction supercloseness estimates. Section 5 establishes local and global gradient recovery superconvergence. Section 6 presents numerical illustrations of the recovered gradient fields and the behavior of a recovery difference on an existing adaptive mesh sequence. Section 7 concludes the paper.

2 Mathematical Model and Finite Element Approximation

Let $\Omega \subset \mathbb{R}^2$ be a bounded polygonal domain. Consider the free vibration of a linearly elastic, isotropic body subject to homogeneous Dirichlet (fixed) boundary conditions. Let $\boldsymbol{u} = (u_1, u_2)^T$ denote the displacement vector, let $\rho > 0$ be the material density, and let λ_L and μ be the Lamé parameters. To distinguish the first Lamé parameter

from the eigenvalue, we denote the former by λ_L and the elasticity eigenvalue by λ. Throughout this paper, the spatial dimension is $d = 2$, and the material density ρ and the Lamé parameters μ, λ_L are fixed constants satisfying $\rho > 0, \mu > 0, 2\mu + d\lambda_L > 0$. The constant C used below may depend on the domain and the fixed material parameters, but is independent of the mesh size h. For any displacement field $\boldsymbol{u}$, the strain tensor is defined by $\varepsilon(\boldsymbol{u}) = \frac{1}{2}\left(\nabla \boldsymbol{u} + (\nabla \boldsymbol{u})^T\right)$, and the stress tensor satisfies the generalized form of Hooke's law $\sigma(\boldsymbol{u}) = 2\mu\varepsilon(\boldsymbol{u}) + \lambda_L \operatorname{div} \boldsymbol{u}\, I$. Here, I is the $d \times d$ identity matrix. The corresponding linear elasticity operator is defined by $\mathcal{L}\boldsymbol{u} := -\operatorname{div} \sigma(\boldsymbol{u})$. For constant Lamé parameters,

$$\mathcal{L}\boldsymbol{u} = -\mu\Delta\boldsymbol{u} - (\lambda_L + \mu)\nabla(\operatorname{div} \boldsymbol{u}).$$

We consider the following linear elasticity eigenvalue problem with homogeneous Dirichlet boundary conditions: find an eigenvalue $\lambda \in \mathbb{R}$ and a corresponding nonzero eigenfunction $\boldsymbol{u}$ such that

$$\begin{cases} -\operatorname{div} \sigma(\boldsymbol{u}) = \lambda\rho\boldsymbol{u}, & x \in \Omega, \\ \qquad\qquad \boldsymbol{u} = \boldsymbol{0}, & x \in \partial\Omega. \end{cases} \tag{2.1}$$

Here, $\lambda = \omega^2$, where ω is the natural angular frequency of the elastic body. Define the energy space $V = [H_0^1(\Omega)]^2$. For any $\boldsymbol{u}, \boldsymbol{v} \in V$, define the bilinear form $a(\boldsymbol{u}, \boldsymbol{v}) = \int_\Omega \sigma(\boldsymbol{u}) : \varepsilon(\boldsymbol{v})\, dx$, and the mass bilinear form $b(\boldsymbol{u}, \boldsymbol{v}) = \int_\Omega \rho\boldsymbol{u} \cdot \boldsymbol{v}\, dx$. By the definition of the stress tensor, $a(\boldsymbol{u}, \boldsymbol{v}) = \int_\Omega [2\mu\varepsilon(\boldsymbol{u}) : \varepsilon(\boldsymbol{v}) + \lambda_L(\operatorname{div} \boldsymbol{u})(\operatorname{div} \boldsymbol{v})]\, dx$. Taking an arbitrary test function $\boldsymbol{v} \in V$, multiplying the first equation in the strong formulation (2.1) by $\boldsymbol{v}$, and integrating over Ω, we obtain $\int_\Omega (-\operatorname{div} \sigma(\boldsymbol{u})) \cdot \boldsymbol{v}\, dx = \lambda \int_\Omega \rho\boldsymbol{u} \cdot \boldsymbol{v}\, dx$. Since $\sigma(\boldsymbol{u})$ is symmetric, $\sigma(\boldsymbol{u}) : \nabla\boldsymbol{v} = \sigma(\boldsymbol{u}) : \varepsilon(\boldsymbol{v})$, and Green's formula gives

$$\int_\Omega (-\operatorname{div} \sigma(\boldsymbol{u})) \cdot \boldsymbol{v}\, dx = \int_\Omega \sigma(\boldsymbol{u}) : \varepsilon(\boldsymbol{v})\, dx - \int_{\partial\Omega} (\sigma(\boldsymbol{u})\boldsymbol{n}) \cdot \boldsymbol{v}\, ds. \tag{2.2}$$

Since $\boldsymbol{v}|_{\partial\Omega} = 0$, the boundary term vanishes, yielding the weak formulation of the continuous eigenvalue problem: find $(\lambda, \boldsymbol{u}) \in \mathbb{R} \times V, \boldsymbol{u} \neq \boldsymbol{0}$ such that

$$a(\boldsymbol{u}, \boldsymbol{v}) = \lambda b(\boldsymbol{u}, \boldsymbol{v}), \qquad \forall \boldsymbol{v} \in V. \tag{2.3}$$

We next state the basic properties required for the subsequent analysis. Assume that the material parameters satisfy the positive definiteness condition for the elastic energy, namely, in two- or three-dimensional linear isotropic elasticity, $\mu > 0, 2\mu + d\lambda_L > 0$, and assume that $\rho > 0$. By the Cauchy--Schwarz inequality and the boundedness of the elasticity tensor, there exists a constant $C_a > 0$, independent of the mesh size, such that $|a(\boldsymbol{u}, \boldsymbol{v})| \leq C_a \|\boldsymbol{u}\|_{1,\Omega} \|\boldsymbol{v}\|_{1,\Omega}, \forall \boldsymbol{u}, \boldsymbol{v} \in V$. On the other hand, Korn's inequality implies the existence of a constant $C_K > 0$ such that $\|\boldsymbol{v}\|_{1,\Omega} \leq C_K \|\varepsilon(\boldsymbol{v})\|_{0,\Omega}, \forall \boldsymbol{v} \in V$. Consequently, there exists a constant $c_a > 0$ such that $a(\boldsymbol{v}, \boldsymbol{v}) \geq c_a \|\boldsymbol{v}\|_{1,\Omega}^2, \forall \boldsymbol{v} \in V$. Since $\rho > 0$ is a positive constant,

there exist positive constants $c_b, C_b > 0$ such that $c_b\|\boldsymbol{v}\|_{0,\Omega}^2 \leq b(\boldsymbol{v},\boldsymbol{v}) \leq C_b\|\boldsymbol{v}\|_{0,\Omega}^2$. $a(\boldsymbol{u},\boldsymbol{v}) = a(\boldsymbol{v},\boldsymbol{u}), b(\boldsymbol{u},\boldsymbol{v}) = b(\boldsymbol{v},\boldsymbol{u})$, Thus, problem (2.3) is a standard symmetric self-adjoint elliptic eigenvalue problem.

By the compact embedding

$$[H_0^1(\Omega)]^d \hookrightarrow [L^2(\Omega)]^d \tag{2.4}$$

and standard self-adjoint spectral theory, the continuous eigenvalue problem (2.3) admits a discrete sequence of positive eigenvalues $0 < \lambda_1 \leq \lambda_2 \leq \cdots, \lambda_j \to +\infty$. The corresponding eigenfunctions can be chosen to be orthonormal with respect to the mass bilinear form $b(\cdot,\cdot)$, i.e., $b(\boldsymbol{u}_i,\boldsymbol{u}_j) = \delta_{ij}$. For the subsequent finite element approximation analysis, we also consider the source problem associated with (2.3).

For any $\boldsymbol{f} \in [L^2(\Omega)]^d$, find $\boldsymbol{w} \in V$, such that

$$a(\boldsymbol{w},\boldsymbol{v}) = b(\boldsymbol{f},\boldsymbol{v}), \qquad \forall \boldsymbol{v} \in V. \tag{2.5}$$

Since the bilinear form $a(\cdot,\cdot)$ is continuous and coercive on V, the Lax--Milgram theorem guarantees that problem (2.5) has a unique solution satisfying the stability estimate $\|\boldsymbol{w}\|_{1,\Omega} \leq C\|\boldsymbol{f}\|_{0,\Omega}$. Define the continuous solution operator $T : [L^2(\Omega)]^d \longrightarrow V$ by

$$T\boldsymbol{f} = \boldsymbol{w}. \tag{2.6}$$

When the domain Ω and the material parameters satisfy the appropriate elliptic regularity conditions, there exists $0 < s \leq 1$ such that $\|T\boldsymbol{f}\|_{1+s,\Omega} \leq C\|\boldsymbol{f}\|_{0,\Omega}$. In the case of full H^2 regularity, one can take $s = 1$, yielding $\|T\boldsymbol{f}\|_{2,\Omega} \leq C\|\boldsymbol{f}\|_{0,\Omega}$. The regularity index s depends on the geometry of the domain and the material parameters. Full H^2 regularity generally cannot be assumed for nonconvex polygonal domains with reentrant corners. The subsequent superconvergence analysis is carried out under stronger smoothness and mesh structure assumptions. By (2.6) and the compact embedding (2.4), T is compact as an operator $[L^2(\Omega)]^d \longrightarrow [L^2(\Omega)]^d$.

Hence, $a(\boldsymbol{u},\boldsymbol{v}) = \lambda a(T\boldsymbol{u},\boldsymbol{v}), \forall \boldsymbol{v} \in V$, and uniqueness of the solution to the source problem gives $\lambda T\boldsymbol{u} = \boldsymbol{u}$. Thus, the original differential eigenvalue problem is equivalent to the spectral problem for the compact operator T. This formulation provides the theoretical basis for the finite element spectral approximation analysis below Boffi (2010).

2.1 Linear Finite Element Discretization and A Priori Error Estimates

Let $\mathcal{T}_h = \{K\}$ be a shape-regular and quasi-uniform family of meshes of the domain Ω. In two dimensions, $\mathcal{T}_h$ is a triangulation. Set $h_K = \operatorname{diam} K, h = \max_{K\in\mathcal{T}_h} h_K$.

Define the continuous piecewise linear vector-valued finite element spaceBrenner and Scott (2002)

$$V_h = \left\{\boldsymbol{v}_h \in V : \boldsymbol{v}_h|_K \in [P_1(K)]^d, \quad \forall K \in \mathcal{T}_h\right\}.$$

Clearly, $V_h \subset V$. The finite element discretization of the continuous problem (2.3) is as follows: find $(\lambda_h, \boldsymbol{u}_h) \in \mathbb{R} \times V_h, \boldsymbol{u}_h \neq \boldsymbol{0}$, such that

$$a(\boldsymbol{u}_h, \boldsymbol{v}_h) = \lambda_h b(\boldsymbol{u}_h, \boldsymbol{v}_h), \qquad \forall \boldsymbol{v}_h \in V_h. \tag{2.7}$$

The mass normalization conditions are usually imposed: $b(\boldsymbol{u}, \boldsymbol{u}) = 1, b(\boldsymbol{u}_h, \boldsymbol{u}_h) = 1$. Let $\{\boldsymbol{\phi}_i\}_{i=1}^N$ be a basis for V_h, and write $\boldsymbol{u}_h = \sum_{j=1}^N U_j \boldsymbol{\phi}_j$. With $\boldsymbol{v}_h = \boldsymbol{\phi}_i$, equation (2.7) becomes the generalized matrix eigenvalue problem

$$KU = \lambda_h MU, \tag{2.8}$$

where the stiffness and mass matrices are defined, respectively, by $K_{ij} = a(\boldsymbol{\phi}_j, \boldsymbol{\phi}_i)$, $M_{ij} = b(\boldsymbol{\phi}_j, \boldsymbol{\phi}_i)$. After imposing the homogeneous Dirichlet boundary conditions and eliminating the constrained degrees of freedom, both the stiffness matrix K and the mass matrix M are symmetric positive definite on the unconstrained degrees of freedom.

Corresponding to the continuous source problem (2.5), the discrete source problem is defined as follows: for any $\boldsymbol{f} \in [L^2(\Omega)]^d$, find $\boldsymbol{w}_h \in V_h$, such that

$$a(\boldsymbol{w}_h, \boldsymbol{v}_h) = b(\boldsymbol{f}, \boldsymbol{v}_h), \qquad \forall \boldsymbol{v}_h \in V_h. \tag{2.9}$$

The coercivity of $a(\cdot, \cdot)$ guarantees that problem (2.9) has a unique solution.

Define the discrete solution operator $T_h : [L^2(\Omega)]^d \longrightarrow V_h$ by $T_h \boldsymbol{f} = \boldsymbol{w}_h$. The continuous and discrete source problems yield Galerkin orthogonality:

$$a(T\boldsymbol{f} - T_h \boldsymbol{f}, \boldsymbol{v}_h) = 0, \qquad \forall \boldsymbol{v}_h \in V_h. \tag{2.10}$$

Suppose that $T\boldsymbol{f} \in [H^{1+s}(\Omega)]^d, 0 < s \leq 1$. By the result in Ciarlet (1991), namely, Céa's lemma (Theorem 13.1), and the standard finite element interpolation error estimate, we have

$$\|T\boldsymbol{f} - T_h \boldsymbol{f}\|_{1,\Omega} \leq Ch^s \|T\boldsymbol{f}\|_{1+s,\Omega}. \tag{2.11}$$

Since the linear elasticity eigenvalue problem is a symmetric self-adjoint elliptic eigenvalue problem, the Aubin--Nitsche duality argument yields an L^2 error estimate for the finite element solution under standard elliptic regularity assumptions. If the corresponding dual problem has $H^{1+\tau}$ regularity, with $0 < \tau \leq 1$, and its solution satisfies the corresponding regularity estimate, then

$$\|T\boldsymbol{f} - T_h \boldsymbol{f}\|_{0,\Omega} \leq Ch^{s+\tau} \|T\boldsymbol{f}\|_{1+s,\Omega}. \tag{2.12}$$

In the case of full H^2 regularity with $s = \tau = 1$, the regularity estimate for the source problem further gives

$$\|T\boldsymbol{f} - T_h \boldsymbol{f}\|_{1,\Omega} \leq Ch \|\boldsymbol{f}\|_{0,\Omega}, \qquad \|T\boldsymbol{f} - T_h \boldsymbol{f}\|_{0,\Omega} \leq Ch^2 \|\boldsymbol{f}\|_{0,\Omega}.$$

Céa's lemma, the interpolation estimates, and the Aubin--Nitsche duality estimates used here are classical results in finite element theory and are invoked without proof.

For the discrete eigenvalue problem, the definition of T_h gives, as in the continuous case, $\lambda_h T_h \boldsymbol{u}_h = \boldsymbol{u}_h$. Thus, the continuous and discrete eigenvalue problems are equivalent, respectively, to $\lambda T \boldsymbol{u} = \boldsymbol{u}, \lambda_h T_h \boldsymbol{u}_h = \boldsymbol{u}_h$. This places finite element eigenvalue approximation within the classical spectral approximation framework for compact self-adjoint operators.

We next invoke the standard Babuška--Osborn theory of finite element spectral approximation Babuška and Osborn (1991).

Let λ be a simple eigenvalue of problem (2.3), and let u and u_h be the corresponding continuous and discrete eigenfunctions, normalized by $b(u,u) = b(u_h,u_h) = 1$. Since eigenfunctions are determined only up to sign, choose the sign of u_h so that $b(u,u_h) \geq 0$. Assume further that the continuous eigenfunction satisfies

$$\boldsymbol{u} \in [H^{1+s}(\Omega)]^d, \qquad 0 < s \leq 1. \tag{2.13}$$

Then, for sufficiently small h, there exists a discrete eigenpair $(\lambda_h, \boldsymbol{u}_h)$, corresponding to λ, and a constant $C > 0$, independent of the mesh size h, such that $\|\boldsymbol{u} - \boldsymbol{u}_h\|_{1,\Omega} \leq Ch^s \|\boldsymbol{u}\|_{1+s,\Omega}$.

If the corresponding dual source problem has $H^{1+\tau}$ regularity, where $0 < \tau \leq 1$, and its solution satisfies the regularity estimate

$$\|z\|_{1+\tau,\Omega} \leq C\|g\|_{0,\Omega}, \qquad g \in [L^2(\Omega)]^d,$$

then standard finite element spectral approximation theory further gives

$$\|u - u_h\|_{0,\Omega} \leq Ch^{s+\tau}. \tag{2.14}$$

Here, z is the solution of the dual source problem with right-hand side g, i.e., it satisfies $a(v,z) = (g,v)_{0,\Omega}, \forall v \in V$. The eigenvalue error also satisfies $|\lambda_h - \lambda| \leq Ch^{2s}$. In particular, in the standard smooth case with $s = 1, \tau = 1$, we have

$$\|\boldsymbol{u} - \boldsymbol{u}_h\|_{1,\Omega} \leq Ch, \tag{2.15}$$

$$\|\boldsymbol{u} - \boldsymbol{u}_h\|_{0,\Omega} \leq Ch^2, \tag{2.16}$$

$$|\lambda_h - \lambda| \leq Ch^2. \tag{2.17}$$

These results provide the basic convergence rates for standard linear finite element approximations of eigenfunctions and eigenvalues, and form the basis for the subsequent superconvergence analysis of area-weighted gradient recovery. To simplify notation, vector-valued functions are also denoted by u from Section 3 onward.

3 Area-Weighted Gradient Recovery Operator

Constructing a posteriori error indicators by recovering derivatives or stresses from finite element solutions is a classical approach to finite element postprocessing Zienkiewicz and Zhu (1992). In this paper, the recovery operator is constructed by nodal area-weighted averaging; its precise definition and the required mesh conditions are given below. For the finite element discretization introduced in Section 2, we define a componentwise area-weighted recovery operator, state the mesh assumptions used in the subsequent analysis, and establish its L^2 stability. The supercloseness and superconvergence estimates are proved in Sections 4 and 5, respectively. Let $\mathcal{T}_h$ be a shape-regular triangulation of Ω, and set $h = \max_{K\in\mathcal{T}_h} h_K$. For any node z, denote its patch by $\omega_z = \bigcup_{K\in\mathcal{T}_h, z\in K} K$. Let $K_1, K_2, \cdots, K_m$ be the m elements adjacent to z.

Suppose that two adjacent triangles sharing an edge, K_1 and K_2, form a quadrilateral. If the lengths of its two pairs of opposite sides satisfy $|\ell_1 - \ell_1'| \le Ch^{1+\alpha}, |\ell_2 - \ell_2'| \le Ch^{1+\alpha}$, then K_1 and K_2 are said to form an $O(h^{1+\alpha})$ approximate parallelogram, where $0 < \alpha \le 1$; see Bank and Xu Bank and Xu (2003).

Partition the mesh into a set of regular elements $\mathcal{T}_{1,h}$ and a set of irregular elements $\mathcal{T}_{2,h}$ such that

$$\mathcal{T}_h = \mathcal{T}_{1,h} \cup \mathcal{T}_{2,h}, \qquad \mathcal{T}_{1,h} \cap \mathcal{T}_{2,h} = \varnothing.$$

Here, the elements in $\mathcal{T}_{1,h}$ satisfy the corresponding local approximate parallelogram condition, and $\mathcal{T}_{2,h}$ contains the remaining elements. Set $\Omega_{i,h} = \text{int}\left(\bigcup_{K\in\mathcal{T}_{i,h}} \overline{K}\right), i = 1, 2$. In the regular region, any two adjacent triangles sharing an edge satisfy the $O(h^{1+\alpha})$ approximate parallelogram condition; the irregular region consists of elements that do not satisfy this local structure condition. Assume that there exists a constant $C > 0$, independent of h, such that $|\Omega_{2,h}| \le Ch^{\sigma_0}, 0 < \sigma_0 \le 1$. Assume that the mesh family is shape-regular and quasi-uniform. Set $\alpha_0 = \min\left\{\alpha, \frac{\sigma_0}{2}, \frac{1}{2}\right\}$. Under these mesh conditions, we study the weak superapproximation property of the nodal interpolant and the superconvergence of area-weighted gradient recovery.

For the local error analysis of gradient recovery, let $\mathcal{N}_h^{\text{reg}}$ denote the set of interior nodes satisfying the local mesh conditions in Lemma 5.1 below. Define the regular recovery region by $\Omega_{\text{reg},h} = \text{int}\left(\bigcup_{\substack{K\in\mathcal{T}_h \\ \mathcal{N}(K)\subset\mathcal{N}_h^{\text{reg}}}} \overline{K}\right)$, where $\mathcal{N}(K)$ is the set of vertices of the element K. Denote the region formed by the remaining elements by $\Omega_{\text{bad},h}$. Assume that there exists a constant $C > 0$, independent of h, such that $|\Omega_{\text{bad},h}| \le C(h^{\sigma_0} + h)$. Here, h^{σ_0} controls the area affected by irregular nodes and their patches, whereas h controls the strip of boundary elements.

For any piecewise constant matrix-valued function on $\mathcal{T}_h$, $q_h \in [P_0(\mathcal{T}_h)]^{2\times 2}$, define the area-weighted gradient recovery operator by

$$G_h[q_h](z) = \sum_{j=1}^{m} \frac{|K_j|}{|\omega_z|} q_h|_{K_j}.$$

For piecewise constant scalar-, vector-, and matrix-valued functions, the area-weighted recovery operator is defined componentwise using the same nodal area weights.

Let $\mathcal{N}_h$ be the set of all mesh nodes, and let $\{\phi_z\}_{z\in\mathcal{N}_h}$ be the continuous piecewise linear finite element nodal basis functions. Using the recovered nodal values above, define the recovered function over the entire domain by

$$G_h[q_h](x) = \sum_{z\in\mathcal{N}_h} G_h[q_h](z)\phi_z(x).$$

Set

$$S_h^1 = \left\{ v_h \in C^0(\overline{\Omega}) : v_h|_K \in P_1(K),\ \forall K \in \mathcal{T}_h \right\}.$$

Thus, the area-weighted gradient recovery operator satisfies $G_h : [P_0(\mathcal{T}_h)]^{2\times 2} \longrightarrow [S_h^1]^{2\times 2}$.

Since the linear finite element function u_h is linear on each element, its gradient ∇u_h is constant on each element and therefore belongs to the domain of the recovery operator. For a finite element eigenfunction u_h, define the recovered gradient by $G_h[\nabla u_h] = \left(G_h[\frac{\partial u_{h,i}}{\partial x_j}]\right)_{2\times 2}$.

3.1 Stability of the Recovery Operator

Lemma 3.1 (Stability of the area-weighted recovery operator)**.** *Let $\mathcal{T}_h$ be a shape-regular triangulation of Ω satisfying the quasi-uniformity condition. For any piecewise constant matrix-valued function on $\mathcal{T}_h$, $q_h \in Q_h$, where $Q_h = [P_0(\mathcal{T}_h)]^{2\times 2}$, let G_h be the area-weighted recovery operator defined earlier in this section. Then there exists a constant $C > 0$, independent of the mesh size h, such that*

$$\|G_h[q_h]\|_{0,\Omega} \le C\|q_h\|_{0,\Omega}. \tag{3.1}$$

Here, $\|\cdot\|_{0,\Omega}$ denotes the L^2 norm over Ω.

Proof. By the definition of the area-weighted recovery operator,

$$G_h[q_h](z) = \sum_{K_j\subset\omega_z} \frac{|K_j|}{|\omega_z|} q_h|_{K_j}.$$

Since $\frac{|K_j|}{|\omega_z|} \ge 0$, and $\sum_{K_j\subset\omega_z} \frac{|K_j|}{|\omega_z|} = 1$, the convex combination property gives

$$|G_h[q_h](z)|^2 \leq \sum_{K_j \subset \omega_z} \frac{|K_j|}{|\omega_z|} |q_h|_{K_j}|^2.$$

Multiplying both sides by $|\omega_z|$ and summing over all nodes yields

$$\sum_z |\omega_z||G_h[q_h](z)|^2 \leq \sum_z \sum_{K_j \subset \omega_z} |K_j||q_h|_{K_j}|^2.$$

Since each element belongs to only a bounded number of nodal patches and the mesh is shape-regular, we have

$$\sum_z \sum_{K_j \subset \omega_z} |K_j||q_h|_{K_j}|^2 \leq C \sum_{K \in \mathcal{T}_h} \int_K |q_h|^2 dx.$$

On the other hand, the continuous piecewise linear representation of the recovered function, together with finite-dimensional norm equivalence on the reference triangle, gives

$$\begin{aligned} \|G_h[q_h]\|_{0,\Omega}^2 &\leq C \sum_{K \in \mathcal{T}_h} |K| \sum_{z \in \mathcal{N}(K)} |G_h[q_h](z)|^2 \\ &= C \sum_{z \in \mathcal{N}_h} |\omega_z| \, |G_h[q_h](z)|^2, \end{aligned}$$

where $\mathcal{N}(K)$ denotes the three vertices of K.

Combining this with the preceding weighted nodal estimate yields

$$\|G_h[q_h]\|_{0,\Omega} \leq C \|q_h\|_{0,\Omega}.$$

This completes the proof. □

4 Weak Superapproximation and Supercloseness Estimates

To express the elasticity bilinear form in terms of its components, define the matrices

$$D_1 = \begin{pmatrix} 2\mu + \lambda_L & 0 \\ 0 & \mu \end{pmatrix}, \qquad D_2 = \begin{pmatrix} \mu & 0 \\ 0 & 2\mu + \lambda_L \end{pmatrix},$$

$$D_3 = \begin{pmatrix} 0 & \lambda_L \\ \mu & 0 \end{pmatrix}, \qquad D_4 = \begin{pmatrix} 0 & \mu \\ \lambda_L & 0 \end{pmatrix}.$$

Theorem 4.1 (Weak superapproximation estimate for elasticity)**.** *Suppose that the triangulation $\mathcal{T}_h = \mathcal{T}_{1,h} \cup \mathcal{T}_{2,h}$ satisfies the local approximate parallelogram mesh*

conditions stated above, and that the Lamé parameters μ and λ_L are constant. Here, $0 < \alpha \leq 1$, $0 < \sigma_0 \leq 1$, $|\Omega_{2,h}| \leq Ch^{\sigma_0}$. Let

$$u = (u_1, u_2)^T \in [H^3(\Omega) \cap W^{2,\infty}(\Omega) \cap H_0^1(\Omega)]^2.$$

Denote its linear finite element nodal interpolant by $u_I = (u_{1I}, u_{2I})^T \in V_h$. Then, for any $v_h = (v_{h,1}, v_{h,2})^T \in V_h$, we have

$$|a(u - u_I, v_h)| = \left| \int_\Omega \sigma(u - u_I) : \varepsilon(v_h)\, dx \right| \leq Ch^{1+\alpha_0} \left(\|u\|_{3,\Omega} + \|u\|_{2,\infty,\Omega} \right) \|v_h\|_{1,\Omega}. \tag{4.1}$$

Here, we use $\alpha_0 = \min\{\alpha, \sigma_0/2, 1/2\}$, as defined in Section 3.

Proof. By the definitions of stress and strain, we have

$$\begin{aligned}
I &= \int_\Omega \sigma(u - u_I) : \varepsilon(v_h)\, dx \\
&= \int_\Omega \Bigg[(2\mu + \lambda_L) \frac{\partial(u_1 - u_{1I})}{\partial x_1} \frac{\partial v_{h,1}}{\partial x_1} + \lambda_L \frac{\partial(u_2 - u_{2I})}{\partial x_2} \frac{\partial v_{h,1}}{\partial x_1} \\
&\quad + \mu \frac{\partial(u_1 - u_{1I})}{\partial x_2} \frac{\partial v_{h,1}}{\partial x_2} + \mu \frac{\partial(u_1 - u_{1I})}{\partial x_2} \frac{\partial v_{h,2}}{\partial x_1} \\
&\quad + \mu \frac{\partial(u_2 - u_{2I})}{\partial x_1} \frac{\partial v_{h,1}}{\partial x_2} + \mu \frac{\partial(u_2 - u_{2I})}{\partial x_1} \frac{\partial v_{h,2}}{\partial x_1} \\
&\quad + (2\mu + \lambda_L) \frac{\partial(u_2 - u_{2I})}{\partial x_2} \frac{\partial v_{h,2}}{\partial x_2} + \lambda_L \frac{\partial(u_1 - u_{1I})}{\partial x_1} \frac{\partial v_{h,2}}{\partial x_2} \Bigg] dx.
\end{aligned}$$

Since v_h is linear on each element $K \in \mathcal{T}_h$, its first derivatives are constant within the element. Applying Green's formula on each element and denoting the outward unit normal to ∂K by $n = (n_1, n_2)^T$, we obtain

$$\begin{aligned}
I = \sum_{K \in \mathcal{T}_h} \Bigg[&\int_{\partial K} (2\mu + \lambda_L)(u_1 - u_{1I}) \frac{\partial v_{h,1}}{\partial x_1} n_1\, ds + \int_{\partial K} \lambda_L (u_2 - u_{2I}) \frac{\partial v_{h,1}}{\partial x_1} n_2\, ds \\
&+ \int_{\partial K} \mu (u_1 - u_{1I}) \frac{\partial v_{h,1}}{\partial x_2} n_2\, ds + \int_{\partial K} \mu (u_1 - u_{1I}) \frac{\partial v_{h,2}}{\partial x_1} n_2\, ds \\
&+ \int_{\partial K} \mu (u_2 - u_{2I}) \frac{\partial v_{h,1}}{\partial x_2} n_1\, ds + \int_{\partial K} \mu (u_2 - u_{2I}) \frac{\partial v_{h,2}}{\partial x_1} n_1\, ds \\
&+ \int_{\partial K} (2\mu + \lambda_L)(u_2 - u_{2I}) \frac{\partial v_{h,2}}{\partial x_2} n_2\, ds + \int_{\partial K} \lambda_L (u_1 - u_{1I}) \frac{\partial v_{h,2}}{\partial x_2} n_1\, ds \Bigg].
\end{aligned}$$

By the definitions of D_1, D_2, D_3, D_4, the preceding expression can be written as

$$I = \sum_{K\in\mathcal{T}_h} \Bigg[\int_{\partial K} (u_1 - u_{1I}) \nabla v_{h,1} \cdot D_1 n \, ds + \int_{\partial K} (u_2 - u_{2I}) \nabla v_{h,2} \cdot D_2 n \, ds + \int_{\partial K} (u_2 - u_{2I}) \nabla v_{h,1} \cdot D_3 n \, ds + \int_{\partial K} (u_1 - u_{1I}) \nabla v_{h,2} \cdot D_4 n \, ds \Bigg]. \tag{4.2}$$

For each boundary term in (4.2), let e denote the corresponding interpolation error component and let v_h denote the corresponding component of the finite element test function. Since v_h is linear on each element and the matrices D_i are constant, elementwise integration by parts gives

$$\sum_{K\in\mathcal{T}_h} \int_{\partial K} e \, \nabla v_h \cdot D_i n_K \, ds = \sum_{K\in\mathcal{T}_h} \int_K \nabla e \cdot D_i^T \nabla v_h \, dx.$$

We decompose $D_i^T = S_i + A_i, S_i = \frac{D_i^T + D_i}{2}, A_i = \frac{D_i^T - D_i}{2}$. Then S_i is symmetric and A_i is skew-symmetric. For $i = 1, 2$, we have $A_i = 0$.

For $i = 3, 4$, since the spatial dimension is two, there exists a constant κ_i such that

$$A_i = \kappa_i \begin{pmatrix} 0 & 1 \\ -1 & 0 \end{pmatrix}.$$

For any scalar interpolation error $e \in H_0^1(\Omega)$ and any continuous piecewise linear scalar function $v_h \in S_h^1 \cap H_0^1(\Omega)$, the skew-symmetric contribution satisfies

$$\sum_{K\in\mathcal{T}_h} \int_K \nabla e \cdot A_i \nabla v_h \, dx = 0.$$

Indeed, since ∇v_h is constant on each element,

$$\mathrm{div}(A_i \nabla v_h) = 0 \quad \text{in each } K.$$

Consequently,

$$\sum_{K\in\mathcal{T}_h} \int_K \nabla e \cdot A_i \nabla v_h \, dx = \sum_{K\in\mathcal{T}_h} \int_{\partial K} e (A_i \nabla v_h) \cdot n_K \, ds.$$

The contributions from interior edges cancel because e is continuous and the tangential derivative of v_h is single-valued on each interior edge. The boundary contributions vanish because $e = 0$ on $\partial\Omega$.

It follows that the four terms in (4.2) can be estimated using the symmetric matrices S_i only. The matrices S_i are constant and uniformly bounded, and their jumps across adjacent elements are zero. Therefore, the assumptions of Lemma

2.1 in Xu and Zhang Xu and Zhang (2004) are satisfied. Applying that lemma to each of the four terms yields (4.3)--(4.6).

$$\left| \sum_{K \in \mathcal{T}_h} \int_{\partial K} (u_1 - u_{1I}) \nabla v_{h,1} \cdot D_1 n \, ds \right| \leq C h^{1+\alpha_0} \left(\|u_1\|_{3,\Omega} + \|u_1\|_{2,\infty,\Omega} \right) |v_{h,1}|_{1,\Omega}, \quad (4.3)$$

$$\left| \sum_{K \in \mathcal{T}_h} \int_{\partial K} (u_2 - u_{2I}) \nabla v_{h,2} \cdot D_2 n \, ds \right| \leq C h^{1+\alpha_0} \left(\|u_2\|_{3,\Omega} + \|u_2\|_{2,\infty,\Omega} \right) |v_{h,2}|_{1,\Omega}, \quad (4.4)$$

$$\left| \sum_{K \in \mathcal{T}_h} \int_{\partial K} (u_2 - u_{2I}) \nabla v_{h,1} \cdot D_3 n \, ds \right| \leq C h^{1+\alpha_0} \left(\|u_2\|_{3,\Omega} + \|u_2\|_{2,\infty,\Omega} \right) |v_{h,1}|_{1,\Omega}, \quad (4.5)$$

$$\left| \sum_{K \in \mathcal{T}_h} \int_{\partial K} (u_1 - u_{1I}) \nabla v_{h,2} \cdot D_4 n \, ds \right| \leq C h^{1+\alpha_0} \left(\|u_1\|_{3,\Omega} + \|u_1\|_{2,\infty,\Omega} \right) |v_{h,2}|_{1,\Omega}. \quad (4.6)$$

Substituting (4.3)--(4.6) into (4.2) and applying the triangle inequality, we obtain

$$\begin{aligned} |a(u - u_I, v_h)| &= \left| \int_\Omega \sigma(u - u_I) : \varepsilon(v_h) \, dx \right| \\ &\leq C h^{1+\alpha_0} \left(\|u_1\|_{3,\Omega} + \|u_1\|_{2,\infty,\Omega} \right) \left(|v_{h,1}|_{1,\Omega} + |v_{h,2}|_{1,\Omega} \right) \\ &\quad + C h^{1+\alpha_0} \left(\|u_2\|_{3,\Omega} + \|u_2\|_{2,\infty,\Omega} \right) \left(|v_{h,1}|_{1,\Omega} + |v_{h,2}|_{1,\Omega} \right) \\ &\leq C h^{1+\alpha_0} \left(\|u\|_{3,\Omega} + \|u\|_{2,\infty,\Omega} \right) \|v_h\|_{1,\Omega}. \end{aligned}$$

This proves (4.1). □

4.1 Supercloseness between the Finite Element Eigenfunction and the Nodal Interpolant

Theorem 4.2 (Supercloseness between the finite element eigenfunction and the nodal interpolant)**.** *Let* (λ, u) *and* (λ_h, u_h) *be corresponding eigenpairs of the continuous and discrete linear elasticity eigenvalue problems, respectively, where* λ *is a simple eigenvalue. Assume that the continuous and discrete eigenfunctions satisfy* $b(u,u) = b(u_h, u_h) = 1$*, and choose the sign of* u_h *so that* $b(u, u_h) \geq 0$*. Suppose that the mesh and regularity conditions of Theorem 4.1 hold, and that the corresponding dual problem has full* H^2 *regularity, so that the error estimates in Section 2 give* $\|u - u_h\|_{0,\Omega} \leq C h^2, |\lambda - \lambda_h| \leq C h^2$*. Then*

$$\|u_h - u_I\|_{1,\Omega} \leq C h^{1+\alpha_0}. \quad (4.7)$$

Proof. Set $w = Tu, w_h = T_h u$, and let $w_I = (Tu)_I$ be the piecewise linear nodal interpolant of w. By the definitions of the continuous and discrete source problems,

$$a(w, v_h) = b(u, v_h), a(w_h, v_h) = b(u, v_h), \forall v_h \in V_h,$$

and hence (2.10) gives $a(w - w_h, v_h) = 0, \forall v_h \in V_h$.

Set $\xi_h = w_h - w_I$. Taking $v_h = \xi_h$ yields

$$\begin{aligned} a(\xi_h, \xi_h) &= a(w_h - w_I, \xi_h) \\ &= a(w - w_I, \xi_h) + a(w_h - w, \xi_h) \\ &= a(w - w_I, \xi_h). \end{aligned}$$

By Theorem 4.1,

$$\begin{aligned} a(\xi_h, \xi_h) &= a(w - w_I, \xi_h) \\ &\leq |a(w - w_I, \xi_h)| \\ &\leq Ch^{1+\alpha_0} \left(\|w\|_{3,\Omega} + \|w\|_{2,\infty,\Omega} \right) \|\xi_h\|_{1,\Omega}. \end{aligned}$$

The coercivity of $a(\cdot, \cdot)$ gives

$$\|\xi_h\|_{1,\Omega} \leq Ch^{1+\alpha_0} \left(\|w\|_{3,\Omega} + \|w\|_{2,\infty,\Omega} \right).$$

Moreover, the identity $\lambda T u = u$, implies $w = \lambda^{-1} u$, and therefore

$$\|T_h u - (Tu)_I\|_{1,\Omega} \leq Ch^{1+\alpha_0}.$$

Using the operator formulations of the continuous and discrete eigenvalue problems, $\lambda T u = u, \lambda_h T_h u_h = u_h$, and the linearity of the interpolation operator, we have $u_I = (\lambda T u)_I = \lambda (Tu)_I$.

Consequently,

$$\begin{aligned} \|u_h - u_I\|_{1,\Omega} &= \|\lambda_h T_h u_h - \lambda (Tu)_I\|_{1,\Omega} \\ &\leq \|\lambda_h T_h u_h - \lambda T_h u\|_{1,\Omega} + \|\lambda T_h u - \lambda (Tu)_I\|_{1,\Omega} \\ &\leq |\lambda_h - \lambda| \|T_h u_h\|_{1,\Omega} + \lambda \|T_h (u_h - u)\|_{1,\Omega} \\ &\quad + \lambda \|T_h u - (Tu)_I\|_{1,\Omega}. \end{aligned}$$

By the stability of the discrete solution operator T_h, $\|T_h f\|_{1,\Omega} \leq C \|f\|_{0,\Omega}$, and the normalization $b(u_h, u_h) = 1$, we obtain $\|T_h u_h\|_{1,\Omega} \leq C$.

$$\|u_h - u_I\|_{1,\Omega} \leq C \left(|\lambda_h - \lambda| + \|u_h - u\|_{0,\Omega} + \|T_h u - (Tu)_I\|_{1,\Omega} \right).$$

By (2.16), (2.17), and the supercloseness estimate for the source problem established above,

$$\begin{aligned} \|u_h - u_I\|_{1,\Omega} &\leq C \left(h^2 + h^2 + h^{1+\alpha_0} \right) \\ &\leq Ch^{1+\alpha_0}. \end{aligned}$$

This proves (4.7). □

5 Local and Global Superconvergence Analysis

For gradient recovery on approximate parallelogram meshes, Xu and Zhang studied the superconvergence of recovery methods, including area-weighted averaging, for linear finite elements Xu and Zhang (2004). For anisotropic meshes, Cao further analyzed the superconvergence of local weighted averaging, local L^2 projection, and least-squares recovery methods Cao (2014). For linear elasticity finite element problems, Shi, Xu, and Zhang studied stress recovery and recovery-based a posteriori error estimation on quadrilateral meshes and established corresponding superconvergence results Shi et al. (2008). These studies provide relevant theoretical background for the analysis of the area-weighted gradient recovery method considered here. The local accuracy of area-weighted recovery depends on the geometry of nodal patches. We therefore state the required assumptions explicitly in terms of a nodal moment condition for quadratic polynomials and prove the corresponding local estimate.

Lemma 5.1 (Local superconvergence of the recovered interpolation gradient)**.** *Let z be an interior node and ω_z its element patch. Assume that the mesh family is shape-regular and quasi-uniform, and let $0 < h \leq 1$. For any symmetric matrix $H \in \mathbb{R}^{2\times 2}$, set $p_H(x) = \frac{1}{2}(x-z)^T H(x-z)$. Assume that there exists a constant $C > 0$, independent of h, z, H, such that*

$$\left| \sum_{K \ni z} \frac{|K|}{|\omega_z|} \big(\nabla I_h p_H\big)|_K \right| \leq C h^{1+\alpha} |H|, \qquad 0 < \alpha \leq 1,$$

where I_h is the piecewise linear nodal interpolation operator, $|H|$ denotes the Frobenius norm of H, and $|\cdot|$ denotes the Euclidean norm for vectors. If $u \in [W^{3,\infty}(\omega_z)]^2$, then its nodal interpolant u_I satisfies

$$\begin{aligned} |G_h[\nabla u_I](z) - \nabla u(z)| &\leq C\left(h^{1+\alpha}|u|_{2,\infty,\omega_z} + h^2 |u|_{3,\infty,\omega_z}\right) \\ &\leq C h^{1+\alpha} \|u\|_{3,\infty,\omega_z}. \end{aligned} \tag{5.1}$$

Proof. First consider a scalar component of u, also denoted by u. A second-order Taylor expansion at the interior node z gives

$$u(x) = u(z) + \nabla u(z)\cdot(x-z) + \frac{1}{2}(x-z)^T D^2 u(z)(x-z) + R_z(x).$$

For any element K containing z, the line segment from z to any of its vertices lies within K. Thus, at every vertex of the patch,

$$|R_z(x)| \leq C h^3 |u|_{3,\infty,\omega_z}.$$

Nodal interpolation reproduces affine functions exactly, and the area weights sum to 1. Therefore, area-weighted recovery also reproduces the gradients of affine

functions exactly. The quadratic term corresponds to $H = D^2u(z)$ and satisfies $\nabla p_H(z) = 0$. The moment condition assumed in the lemma then gives

$$|G_h[\nabla I_h p_H](z)| \le Ch^{1+\alpha}|u|_{2,\infty,\omega_z}.$$

We next estimate the remainder. Denote the three vertices of K by a_1, a_2, a_3, and the corresponding local nodal basis functions by ϕ_1, ϕ_2, ϕ_3. Shape regularity and quasi-uniformity imply $|\nabla\phi_i| \le Ch^{-1}$, and hence

$$\begin{aligned}\left|(\nabla I_h R_z)|_K\right| &= \left|\sum_{i=1}^{3} R_z(a_i)\nabla\phi_i\right| \\ &\le \sum_{i=1}^{3} |R_z(a_i)|\,|\nabla\phi_i| \\ &\le Ch^2|u|_{3,\infty,\omega_z}.\end{aligned}$$

Since the area weights are nonnegative and sum to 1, we further obtain

$$|G_h[\nabla I_h R_z](z)| \le Ch^2|u|_{3,\infty,\omega_z}.$$

By the linearity of the interpolation and recovery operators, combining the preceding estimates for the affine term, quadratic term, and remainder yields

$$|G_h[\nabla u_I](z) - \nabla u(z)| \le C\left(h^{1+\alpha}|u|_{2,\infty,\omega_z} + h^2|u|_{3,\infty,\omega_z}\right).$$

Since $0 < h \le 1$ and $0 < \alpha \le 1$, we have $h^2 \le h^{1+\alpha}$, which gives the second inequality in (5.1). Applying the argument componentwise to the vector-valued function completes the proof. □

The local quadratic moment condition above is an additional mesh assumption imposed on the patches of regular nodes in this paper. It controls the area-weighted recovery error for the gradients of interpolated quadratic polynomials and does not follow automatically from shape regularity and quasi-uniformity alone. Theorem 5.1 below establishes a global gradient recovery superconvergence estimate under the assumption that this condition holds uniformly at all regular nodes.

Theorem 5.1 (Superconvergence of the recovered finite element gradient)**.** *Let (λ, u) and (λ_h, u_h) be corresponding eigenpairs of the continuous and discrete linear elasticity eigenvalue problems, respectively, where λ is a simple eigenvalue, $u = (u_1, u_2)^T$, and $u_h = (u_{h,1}, u_{h,2})^T \in V_h$. Assume that the continuous and discrete eigenfunctions satisfy $b(u, u) = b(u_h, u_h) = 1$, and choose the sign of u_h so that $b(u, u_h) \ge 0$. Assume that $u \in [H^3(\Omega) \cap W^{3,\infty}(\Omega)]^2$, the triangulation $\mathcal{T}_h$ satisfies the local approximate parallelogram mesh conditions of Theorem 4.1, and the dual regularity condition required in Theorem 4.2 holds. Assume also that the local*

quadratic moment condition in Lemma 5.1 holds with the same exponent α as in Theorem 4.1 and with a uniform constant at all regular nodes. In addition, suppose that the irregular recovery region satisfies the area bound stated in Section 3, $|\Omega_{\mathsf{bad},h}| \le C(h^{\sigma_0} + h)$. Then the area-weighted recovered gradient satisfies

$$\|G_h[\nabla u_h] - \nabla u\|_{0,\Omega} \le Ch^{1+\alpha_0}. \tag{5.2}$$

Here, $G_h[\nabla u_h]$ is the area-weighted recovered gradient of the finite element eigenfunction u_h, α_0 is defined in Theorem 4.1, $\|\cdot\|_{0,\Omega}$ denotes the L^2 norm of matrix-valued functions on Ω, and $C > 0$ is independent of the mesh size h.

Proof. Let $u_I \in V_h$ be the piecewise linear nodal interpolant of the continuous eigenfunction u, and let $(\nabla u)_I$ be the componentwise continuous piecewise linear nodal interpolant of ∇u.

The triangle inequality gives

$$\begin{aligned}
&\|G_h[\nabla u_h] - \nabla u\|_{0,\Omega} \\
&\le \|G_h[\nabla u_h] - G_h[\nabla u_I]\|_{0,\Omega} \\
&\quad + \|G_h[\nabla u_I] - (\nabla u)_I\|_{0,\Omega} \\
&\quad + \|(\nabla u)_I - \nabla u\|_{0,\Omega}.
\end{aligned}$$

We first estimate the first term. By the linearity of the recovery operator, its stability in Lemma 3.1, and the supercloseness estimate in Theorem 4.2, we have

$$\begin{aligned}
&\|G_h[\nabla u_h] - G_h[\nabla u_I]\|_{0,\Omega} \\
&= \|G_h[\nabla(u_h - u_I)]\|_{0,\Omega} \\
&\le C\|\nabla(u_h - u_I)\|_{0,\Omega} \\
&\le C\|u_h - u_I\|_{1,\Omega} \\
&\le Ch^{1+\alpha_0}.
\end{aligned}$$

We next estimate the second term. We use the regular and irregular recovery regions defined in Section 3. By Lemma 5.1, for any regular node $z \in \mathcal{N}_h^{\mathsf{reg}}$, we have

$$|G_h[\nabla u_I](z) - \nabla u(z)| \le Ch^{1+\alpha}\|u\|_{3,\infty,\Omega}.$$

Both $G_h[\nabla u_I]$ and $(\nabla u)_I$ are continuous piecewise linear matrix-valued functions. For any element K in the regular region, denote its three vertices by z_1, z_2, z_3. Then, for any $x \in K$,

$$G_h[\nabla u_I](x) - (\nabla u)_I(x) = \sum_{i=1}^{3} \left(G_h[\nabla u_I](z_i) - \nabla u(z_i)\right) \phi_{z_i}(x).$$

Lemma 5.1, together with the nonnegativity and partition-of-unity property of the nodal basis functions, yields

$$|G_h[\nabla u_I](x) - (\nabla u)_I(x)| \le Ch^{1+\alpha}\|u\|_{3,\infty,\Omega}.$$

$$\|G_h[\nabla u_I] - (\nabla u)_I\|_{0,\Omega_{\mathsf{reg},h}} \le Ch^{1+\alpha}\|u\|_{3,\infty,\Omega}.$$

For any node $z \in \mathcal{N}_h$, including boundary nodes and all vertices of elements in the irregular recovery region, the definition of the area-weighted recovery operator gives

$$\begin{aligned}
&|G_h[\nabla u_I](z) - \nabla u(z)| \\
&= \left| \sum_{K \ni z} \frac{|K|}{|\omega_z|} \left((\nabla u_I)|_K - \nabla u(z) \right) \right| \\
&\le \sum_{K \ni z} \frac{|K|}{|\omega_z|} \left| (\nabla u_I)|_K - \nabla u(z) \right|.
\end{aligned}$$

The standard pointwise gradient interpolation estimate for linear finite elements, together with shape regularity, yields

$$\left| (\nabla u_I)|_K - \nabla u(z) \right| \le Ch\|u\|_{2,\infty,\omega_z}, \qquad K \ni z.$$

Since the area weights are nonnegative and sum to 1, we obtain

$$|G_h[\nabla u_I](z) - \nabla u(z)| \le Ch\|u\|_{2,\infty,\Omega}.$$

We now transfer this nodal estimate to the irregular recovery region. For any element $K \subset \Omega_{\mathsf{bad},h}$, denote its three vertices by z_1, z_2, z_3. Since both $G_h[\nabla u_I]$ and $(\nabla u)_I$ are continuous piecewise linear matrix-valued functions, for any $x \in K$,

$$G_h[\nabla u_I](x) - (\nabla u)_I(x) = \sum_{i=1}^{3} \left(G_h[\nabla u_I](z_i) - \nabla u(z_i) \right) \phi_{z_i}(x),$$

where ϕ_{z_i} denotes the nodal basis function associated with vertex z_i.

Using the nonnegativity and partition-of-unity property of the nodal basis functions, namely $\phi_{z_i}(x) \ge 0, \sum_{i=1}^{3} \phi_{z_i}(x) = 1$, we obtain

$$|G_h[\nabla u_I](x) - (\nabla u)_I(x)| \le Ch\|u\|_{2,\infty,\Omega}.$$

Squaring and integrating over $\Omega_{\mathsf{bad},h}$ gives

$$\begin{aligned}
&\|G_h[\nabla u_I] - (\nabla u)_I\|^2_{0,\Omega_{\mathsf{bad},h}} \\
&= \int_{\Omega_{\mathsf{bad},h}} |G_h[\nabla u_I] - (\nabla u)_I|^2 \, dx \\
&\le Ch^2 |\Omega_{\mathsf{bad},h}| \|u\|^2_{2,\infty,\Omega}.
\end{aligned}$$

Taking the square root, we have

$$\|G_h[\nabla u_I] - (\nabla u)_I\|_{0,\Omega_{\mathsf{bad},h}} \le Ch|\Omega_{\mathsf{bad},h}|^{1/2}\|u\|_{2,\infty,\Omega}.$$

Finally, using the assumed area bound $|\Omega_{\mathsf{bad},h}| \le C(h^{\sigma_0} + h)$, and the inequality $(h^{\sigma_0} + h)^{1/2} \le h^{\sigma_0/2} + h^{1/2}$, we obtain

$$\|G_h[\nabla u_I] - (\nabla u)_I\|_{0,\Omega_{\mathsf{bad},h}} \le C\left(h^{1+\frac{\sigma_0}{2}} + h^{\frac{3}{2}}\right)\|u\|_{2,\infty,\Omega}.$$

Combining the estimates over the regular and irregular regions yields

$$\begin{aligned}
&\|G_h[\nabla u_I] - (\nabla u)_I\|_{0,\Omega} \\
&\le C\Big[h^{1+\alpha}\|u\|_{3,\infty,\Omega} + \left(h^{1+\frac{\sigma_0}{2}} + h^{\frac{3}{2}}\right)\|u\|_{2,\infty,\Omega}\Big] \\
&\le Ch^{1+\alpha_0}\left(\|u\|_{3,\infty,\Omega} + \|u\|_{2,\infty,\Omega}\right),
\end{aligned}$$

where $\alpha_0 = \min\left\{\alpha, \frac{\sigma_0}{2}, \frac{1}{2}\right\}$.

For the third term, the standard piecewise linear interpolation error estimate gives

$$\|(\nabla u)_I - \nabla u\|_{0,\Omega} \le Ch^2\|u\|_{3,\Omega}.$$

The triangle inequality then yields

$$\begin{aligned}
&\|G_h[\nabla u_h] - \nabla u\|_{0,\Omega} \\
&\le \|G_h[\nabla u_h] - G_h[\nabla u_I]\|_{0,\Omega} \\
&\quad + \|G_h[\nabla u_I] - (\nabla u)_I\|_{0,\Omega} \\
&\quad + \|(\nabla u)_I - \nabla u\|_{0,\Omega} \\
&\le Ch^{1+\alpha_0} + Ch^{1+\alpha_0}\left(\|u\|_{3,\infty,\Omega} + \|u\|_{2,\infty,\Omega}\right) \\
&\quad + Ch^2\|u\|_{3,\Omega}.
\end{aligned}$$

Since $0 < h < 1$ and $0 < \alpha_0 \le \frac{1}{2}$, we have $h^2 \le h^{1+\alpha_0}$. Therefore,

$$\|G_h[\nabla u_h] - \nabla u\|_{0,\Omega} \le Ch^{1+\alpha_0}\left(1 + \|u\|_{3,\infty,\Omega} + \|u\|_{2,\infty,\Omega} + \|u\|_{3,\Omega}\right).$$

Since the eigenfunction u is fixed and the regularity norms above are finite and independent of h, these norms can be absorbed into the constant C, yielding

$$\|G_h[\nabla u_h] - \nabla u\|_{0,\Omega} \le Ch^{1+\alpha_0}.$$

This proves (5.2). □

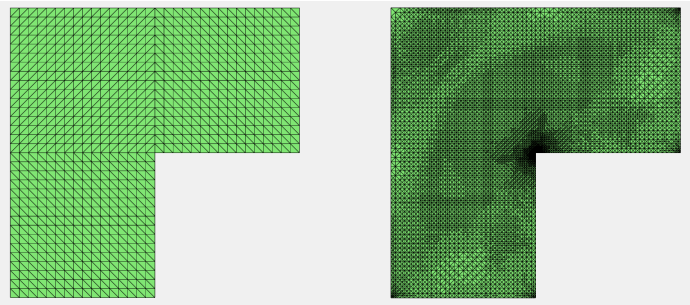
Thus, under the mesh structure assumptions, local quadratic moment condition, area bound on the irregular recovery region, and regularity assumptions of Theorem 5.1, area-weighted gradient recovery has the superconvergence property established above. This result provides the theoretical foundation for the numerical illustrations of the recovered gradient presented in Section 6.

6 Numerical Experiments

6.1 Experimental Setup and Mesh Analysis on the L-Shaped Domain

We reuse an existing adaptive mesh sequence to illustrate area-weighted recovery for the two-dimensional elasticity eigenvalue problem, using the elementwise recovery difference ζ_K defined below. We compare gradient fields and indicator decay; these experiments do not directly verify all assumptions of the superconvergence theorem. Continuous piecewise linear triangular finite elements are used throughout, with material parameters $\mu = 1, \lambda_L = 1, \rho = 1,$ The boundary conditions are the same as in the preceding model: homogeneous Dirichlet conditions are imposed on the entire boundary. The discrete eigenvalue problem uses the mass normalization $b(u_h, u_h) = 1$. The computations focus on the first eigenpair. Gradient recovery is performed using the nodal area-weighted operator defined in Section 3.

The local gradient recovery indicator for adaptive marking is defined by $\zeta_K = \|G_h[\nabla u_h] - \nabla u_h\|_{0,K}$, and the corresponding global indicator is $\zeta = \left(\sum_{K\in\mathcal{T}_h} \zeta_K^2\right)^{1/2}$. The adaptive computation uses Dörfler marking based on ζ_K^2 Dörfler (1996), with marking parameter $\theta = 0.6$. After each finite element eigenpair computation, the recovered gradient $G_h[\nabla u_h]$ is constructed. The elementwise gradient recovery indicators ζ_K are then used to select the elements for refinement, and bisection generates the next mesh. The adaptive experiments are performed on the L-shaped domain $\Omega = (-1, 1)^2 \setminus \big([0, 1] \times [-1, 0]\big)$. This domain has a reentrant corner at the origin $(0, 0)$, near which the continuous eigenfunction may exhibit a singularity that affects the convergence of the finite element approximation. This geometry illustrates localized recovery differences and adaptive refinement. The initial triangulation consists of 6 triangles. To reduce the influence of an excessively coarse initial mesh on the subsequent error distribution, 4 uniform refinements are performed first, yielding 1536 triangles and 833 nodes. After imposing the homogeneous boundary conditions and eliminating the constrained degrees of freedom, the first adaptive computation has 1410 degrees of freedom. At adaptive level 17, the number of degrees of freedom is $N_{\mathsf{dof}} = 246482$.



(a) Initial mesh (b) Adaptive mesh at level 10

Figure 1: Initial mesh and adaptive mesh at level 10 on the L-shaped domain

Figure 1 compares the initial mesh with adaptive level 10 for clarity; indicator decay is evaluated over all 17 levels. Figure 1 shows refinement concentrated near the reentrant corner, with coarser elements farther away and a gradual transition. This indicates that marking driven by the gradient recovery indicator ζ_K can select local refinement regions according to the computed distribution of recovery differences. The computed first eigenfunction is shown in Figure .2.

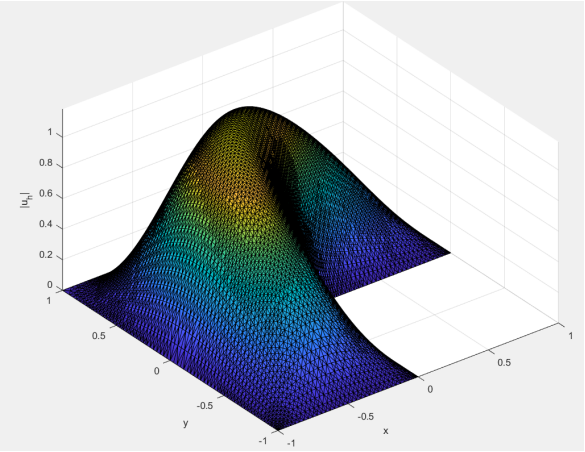


Figure 2: Magnitude $|u_h|$ of the first eigenfunction on the L-shaped domain

The plotted quantity is the magnitude of the discrete displacement vector, defined by $|u_h| = \sqrt{u_{h,1}^2 + u_{h,2}^2}$. The displacement vanishes on the boundary. Its magnitude illustrates the eigenmode distribution but does not establish componentwise accuracy or exclude nonphysical oscillations. For the first eigenfunction at adaptive level 10, Figures .3 and 4 compare the original and recovered gradients using the magnitude of the two displacement derivatives in the

x direction.

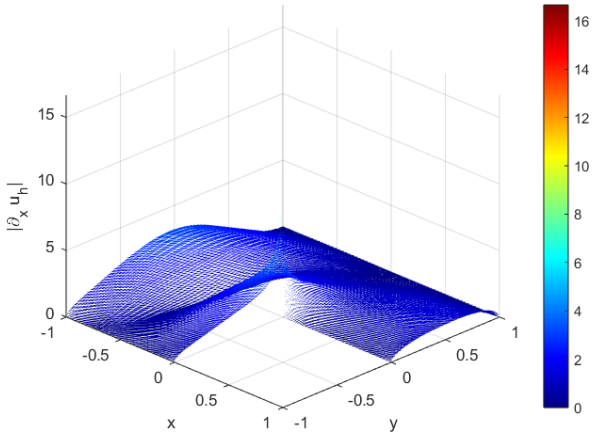


Figure .3: Magnitude $|\partial_x u_h|$ of the original finite element gradient in the x direction on the L-shaped domain

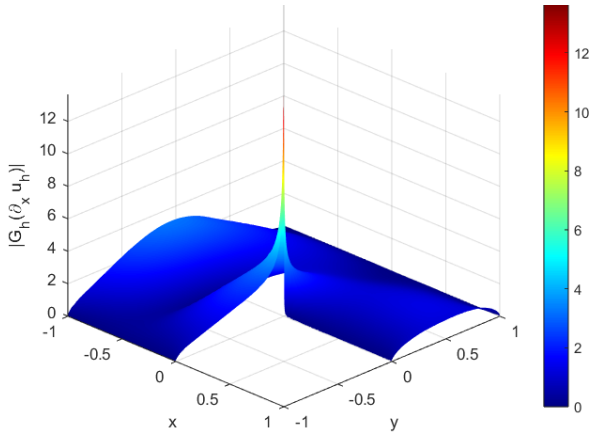


Figure .4: Magnitude of the area-weighted recovered gradient in the x direction on the L-shaped domain

The original gradient in Figure .3 is piecewise constant and discontinuous across elements; recovery produces the continuous field in Figure .4. Both have large magnitudes near the reentrant corner, with a more localized recovered peak. Continuity alone does not establish accuracy relative to the exact gradient. To further examine the differences between the two gradients on individual elements, we use the piecewise linear interpolation of the recovered gradient within each element to compute the elementwise root-mean-square difference in the x-direction

gradient:

$$d_{K,x} = \left(\frac{1}{|K|} \int_K \sum_{i=1}^{2} \left(G_h[\partial_x u_{h,i}] - \partial_x u_{h,i} \right)^2 \, \mathrm{d}x \right)^{1/2}.$$

The resulting spatial distribution is shown in Figure .5. Figure .5 shows recovery differences concentrated near the reentrant corner. The maximum computed elementwise root-mean-square difference is 5.32387670, and the centroid of the corresponding element is approximately $(0.001953,\ 0.000651)$, very close to the reentrant corner of the L-shaped domain. To make the differences on other elements more visible, the 95th percentile is used as the upper limit of the color scale. Values exceeding this limit are displayed using the highest color level, without truncating the original data. The quantity $d_{K,x}$ measures only the gradient recovery differences of the two displacement components in the x direction and is normalized by the element area. It should not be confused with the full gradient recovery indicator ζ_K used for adaptive marking. Recovery retains strong corner variations while smoothing the gradient field. We next examine global recovery differences along the same mesh sequence.

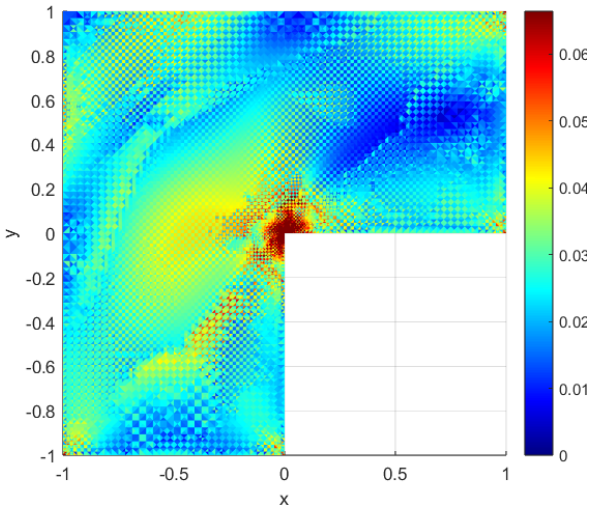


Figure .5: Distribution of gradient recovery differences in the x direction on the L-shaped domain

6.2 Decay of the Gradient Recovery Difference Along the Adaptive Mesh Sequence

To examine the behavior of the gradient recovery difference under adaptive refinement, the same computation is continued for 17 adaptive levels. The

numbers of degrees of freedom and the global gradient recovery differences at each level are listed in Table 1.

Table .1 shows that, as the number of degrees of freedom increases from 1410 to 246482, the global recovery indicator decreases from 3.452254×10^{-1} to 2.191708×10^{-2}. The indicator decreases monotonically throughout refinement.

Table 1: Adaptive computation results on the L-shaped domain

Adaptive level	Degrees of freedom N_{dof}	Global gradient recovery difference ζ
1	1410	3.452254×10^{-1}
2	1714	2.930324×10^{-1}
3	2274	2.420114×10^{-1}
4	2962	2.057396×10^{-1}
5	3920	1.757506×10^{-1}
6	5482	1.525573×10^{-1}
7	7630	1.294636×10^{-1}
8	10474	1.092612×10^{-1}
9	14900	9.005577×10^{-2}
10	20818	7.727658×10^{-2}
11	29934	6.520995×10^{-2}
12	41638	5.441955×10^{-2}
13	59866	4.476945×10^{-2}
14	84218	3.815540×10^{-2}
15	121290	3.219447×10^{-2}
16	170590	2.669911×10^{-2}
17	246482	2.191708×10^{-2}

To further examine the relationship between ζ and the number of degrees of freedom, the results are plotted on logarithmic axes in Figure .6.

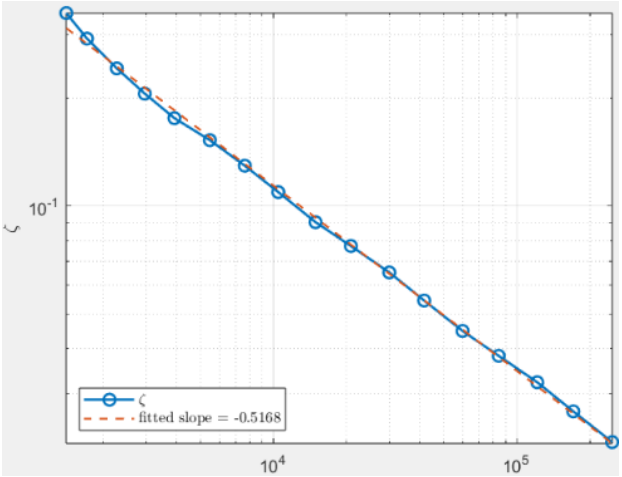


Figure 6: Global gradient recovery difference versus degrees of freedom on the L-shaped domain

Using $\zeta \approx CN_{\text{dof}}^{\beta}$ to fit the results from all 17 levels by least squares gives $\beta = -0.516803$. The results closely follow the fitted power law $\zeta \approx CN_{\text{dof}}^{-0.5168}$. The fitted exponent describes this singular-domain, locally nonuniform mesh sequence, rather than the theoretical superconvergence rate in h established in Section 5 under the local approximate parallelogram mesh conditions. Figures .1 and 6 link corner refinement with decreasing global recovery differences. The adaptive cycle consists of eigenpair solution, gradient recovery, evaluation of ζ_K, element marking, and mesh update. The fitted exponent should not be identified with the theoretical exponent $1 + \alpha_0$ in Theorem 5.1, whose assumptions include the stated quasi-uniformity and local mesh-structure conditions.

References

D. Boffi, Finite element approximation of eigenvalue problems, *Acta Numerica*, 19 (2010), 1--120.

I. Babuška and J. Osborn, Eigenvalue problems, in *Handbook of Numerical Analysis*, Vol. II, North-Holland, Amsterdam, 1991, 641--787.

O. C. Zienkiewicz and J. Z. Zhu, The superconvergent patch recovery and a posteriori error estimates. Part 1: The recovery technique, *International*

Journal for Numerical Methods in Engineering, 33(7) (1992), 1331--1364. doi:10.1002/nme.1620330702.

R. E. Bank and J. Xu, Asymptotically exact a posteriori error estimators, Part I: Grids with superconvergence, *SIAM Journal on Numerical Analysis*, 41(6) (2003), 2294--2312.

J. Xu and Z. Zhang, Analysis of recovery type a posteriori error estimators for mildly structured grids, *Mathematics of Computation*, 73(247) (2004), 1139--1152.

W. Cao, On the superconvergence patch recovery techniques for the linear finite element approximation on anisotropic meshes, *Journal of Computational and Applied Mathematics*, 265 (2014), 33--51. doi:10.1016/j.cam.2013.09.031.

Z.-C. Shi, X. Xu, and Z. Zhang, The patch recovery for finite element approximation of elasticity problems under quadrilateral meshes, *Discrete and Continuous Dynamical Systems -- B*, 9(1) (2008), 163--182. doi:10.3934/dcdsb.2008.9.163.

S. C. Brenner and L. R. Scott, *The Mathematical Theory of Finite Element Methods*, 2nd ed., Springer, New York, 2002.

P. G. Ciarlet, Basic error estimates for elliptic problems, in *Handbook of Numerical Analysis*, Vol. II, North-Holland, Amsterdam, 1991, 17--351.

W. Dörfler, A convergent adaptive algorithm for Poisson's equation, *SIAM Journal on Numerical Analysis*, 33(3) (1996), 1106--1124.

Declaration of AI Use

This manuscript was prepared through the intellectual contributions of the author(s) to the study design, data analysis, interpretation of results, and scholarly content. ChatGPT, Claude and Perplexity were used solely to assist with grammatical refinement and reference formatting during manuscript revision. The author(s) accept full responsibility for the accuracy, integrity, and final content of the manuscript.